Received: Added at production | Revised: Added at production | Accepted: Added at production

DOI: xxx/xxxx

ARTICLE TYPE

A Full Duplex Radio over Fiber Architecture Employing 12 Gbps 16 × 16 Optical MIMO for Next Generation Communication Networks

Saeed Iqbal[1] | Aadil Raza[2] | Muhammad Fasih Uddin Butt*[1] | Salman Ghafoor[3] | Mohammed El-Hajjar[4]

[1]Department of Electrical and Computer Engineering, COMSATS University Islamabad, Islamabad, Pakistan
[2]Department of Physics, COMSATS University Islamabad, Islamabad, Pakistan
[3]School of Electrical Engineering and Computer Science, National University of Sciences and Technology (NUST), Islamabad, Pakistan
[4]School of Electronics and Computer Science, University of Southampton, Southampton, United Kingdom

Correspondence
*Muhammad Fasih Uddin Butt, Department of Electrical and Computer Engineering, COMSATS University Islamabad, Islamabad, Pakistan. Email: fasih@comsats.edu.pk

Present Address
Department of Electrical and Computer Engineering, COMSATS University Islamabad, Islamabad, Pakistan

Summary

In this paper, a full duplex Millimeter Wave (mm-wave) enabled Radio-over-Fiber (RoF) architecture is proposed for Distributed Antenna Systems (DAS). This architecture is capable of achieving transmission of 16 × 16 optical Multiple Input Multiple Output (MIMO) spatial streams at 12 Gbps per spatial stream by employing Wavelength Division Multiplexing (WDM) and exploiting its other degrees of freedom such as polarization states and modes of wavelengths. A single laser source based multi-wavelength comb and wavelength reuse techniques along with Plastic Optical Fiber (POF) are employed to make the proposed architecture cost efficient. Optical heterodyne detection is performed at the Radio Access Unit (RAU) to generate mm-wave carrier frequency at 60 GHz. Channel equalization is achieved for Pulse Amplitute Modulation (PAM-4) data signal by employing Least Mean Square (LMS) equalizer to mitigate the optical fiber channel effects. Our proposed system supports 16 × 12 Gbps for Downlink (DL) and Uplink (UL) transmissions. To evaluate the performance of the proposed system, we compare the receiver sensitivities at FEC limit of 3.8×10^{-3} of Bit Error Ratio (BER) of Back to Back (B2B) system, employing no fiber effects, with its counterparts. We show that acceptable power penalties for the fiber lengths of 200 meter and 400 meter are achieved for both LP01 and LP11 modes in DL and UL directions.

KEYWORDS:
Radio-over-Fiber, Distributed Antenna Systems, Wavelength Division Multiplexing, Plastic Optical Fiber, Radio Access Unit, Millimeter Wave

1 | INTRODUCTION

In recent years, the demand for higher bandwidth and data rate has been increasing exponentially. It has been reported by CISCO that by the end of year 2021, there will be 27.1 billion network devices and 4.6 billion internet users[1]. To meet this unabated demand in future communication networks, several enabling technologies which include, but are not limited to, massive Multiple Input Multiple Output (MIMO)[2], Millimeter Wave (mm-wave) communications[3], cell densification such as Distributed

[0]**Abbreviations:** MMG, MultiMode Generator; MF, Mode Filter; PS, Polarization Splitter; PC, Polarization Coupler; MZM, Mach-Zehnder Modulator; OC, Optical Coupler; OS, Optical Splitter.

Antenna System (DAS)[4] and Radio over Fiber (RoF)[5] are in the phase of research and development. **Similarly, to improves system performance cognitive radio[6] and cross-layer designs for exiting network have been proposed[7,8,9,10]**. However, for next generation communication networks, mm-wave enabled RoF systems may be a potential solution to meet this demand. The mm-wave spectrum provides a wide range of frequencies with larger bandwidth which increases the data rate enormously compared with traditional Radio Frequency (RF) spectrum. However, due to multiple impairments such as atmospheric absorption, free space path loss, scattering of signal due to water molecules and non-line of sight, mm-wave may not support longer distances[3]. Whereas, RoF is a promising technology which provides a reliable solution coupled with large bandwidth optical fiber links. In RoF technology, optical carrier is modulated with the data stream for transmission through optical fiber[5]. The RoF communication technology is based upon the combination of wireless communication and optical communication. The scope of research in RoF communication is moving forward from theoretical study to system development and service applications. This technology is now used to develop electromagnetic interference free, cost-efficient broadband wireless access solutions. The data rate hungry applications such as 3D, 4K video and live streaming for clinical applications require such a high data rate which might not be possible without optical fiber integration in wireless access services. Therefore, RoF based link is a potential alternative solution for indoor short range mm-wave transmission.

The RoF based mm-wave link using higher order modulation schemes can realize higher link capacity[11]. The higher order modulation schemes, such as 64QAM, 16QAM, 8QAM and QPSK etc., require the employment of pre-coding schemes[12,13] for both phase and amplitude to combat the effects of the channel. However, this requires an expensive and complex IQ modulator for the generation of QAM signal. In contrast, Pulse Amplitude Modulation (PAM-4), where information is transmitted by varying only the amplitude of the signal, can be easily employed with intensity modulation rather than using expensive IQ modulator for the generation of QAM/QPSK signal. Recently, PAM-4 has been adopted by IEEE P802.3bs 400 GbE task force because of its higher bandwidth efficiency, lower cost, lower power consumption and less implementation complexity[14,15,16], while employing Intensity Modulation and Direct Detection (IM/DD) systems. PAM-4 signal transmission in RoF technology has been demonstrated experimentally over a distance of 20 km by using SMF and then wireless transmission at 1 meter distance has been achieved at the data rate of 8.4 Gbps[17]. Real time transmission of 4.63 Gbps PAM-4 signal over 25 km SMF has been achieved in[18] by utilizing Cascaded Multi-Modulus-Algorithm (CMMA) equalization and symbol interleaving. Pre-distortion look up table at the transmitter side and CMMA equalization at the receiver side has been employed in[19] for 10 Gbaud PAM-4 signal over 25 km SMF and free space wireless distance of 0.5 meter at 40 GHz. Throughput and wireless transmission distance have been further improved in[20] in which 13 Gbps PAM-4 signal transmission has been demonstrated experimentally at 9 meter wireless distance. Although extensive studies have been carried out for PAM-4 data stream transmission over SMF[21,17,18,19,20,22], the existing architectures do not address PAM-4 optical MIMO transmission which needs to be investigated for short range communication networks as well as for wireless data center networks. Experimental demonstration to achieve MIMO streams has been reported in[23] by using subcarrier multiplexing. However, subcarrier multiplexing and other frequency translation schemes are not bandwidth efficient in RF domain. Additionally, Wavelength Division Multiplexing (WDM) has been used to transmit MIMO streams[24]. However, WDM increases the cost and complexity of the system which is an inherent disadvantage of multiplexing techniques. It implies that for including further wavelengths in the already deployed WDM network, newer laser sources would be required. Also, efficiency of Erbium-Doped Fiber Amplifiers (EDFAs) for these wavelengths is not good because of non flatness in its gain spectrum[25]. However, for Polarization Division Multiplexing (PDM) and Mode Division Multiplexing (MDM), same wavelengths are used and hence do not require large bandwidth EDFAs as well as separate laser sources.

Moreover, MDM has been proposed for Fifth Generation (5G) fronthaul network in 5G-PPP 2nd phase project BlueSPACE[26]. This project, BlueSPACE, has suggested to use MDM in RoF technology to support mm-wave carrier for larger bandwidth. These optical techniques suggested in[26] are compatible with other 5G-PPP 2nd phase projects like 5G-PHOS[27] and Metro-Haul[28]. MDM is a technique that is used to exploit maximum benefits from Multimode Fiber (MMF) in which each Linearly Polarised (LP) mode of MMF works as an independent channel to carry data[29,30]. Further, MDM can be regarded as an optical MIMO channel which helps to improve both the diversity gain and increase the data rate. Moreover, implementing MIMO without MMF will be much more complex and expensive. In the existing transmission schemes, as studied in[31,32,33], the optical carrier is modulated with high frequency RF signals for transportation over silica based optical fiber[16]. For example, to achieve MIMO transmission, multiple laser sources, high frequency local oscillators (LOs) and wide range bandwidth EDFAs will be required to employ such a higher order MIMO system which ultimately make the system complex and less cost efficient. Different cost reduction and performance enhancement techniques have been surveyed and reported in[34] and a few of them have been incorporated in this work to achieve a higher data rate and cost-efficient system. Therefore, in the proposed architecture,

16×16 optical MIMO transmission is achieved by exploiting the polarization states of LP modes of the MMF. In the proposed architecture, the data rate is improved while also reducing the number of electrical and optical components in order to achieve cost efficiency. High frequency LOs and mixers at the transmitter side are avoided because baseband (PAM-4) data transmission is adopted in the proposed scheme, which is simple to implement as compared to complex high order modulation schemes such as QAM and QPSK. Furthermore, multi-wavelength comb source is employed to avoid the use of multiple laser sources and mm-wave (60 GHz) signals is generated by heterodyne detection to avoid expensive high frequency LOs at the RAU. Additionally, Plastic Optical Fiber (POF) instead of silica based fiber is used as a transmission medium, which ultimately reduces the cost. The contribution of this work is the design of PAM-4 based optical mm-wave enabled MIMO transmission to meet 5G throughput demand. To achieve 16×16 optical MIMO transmission, PDM along with MDM and WDM are exploited in Graded Index Plastic Optical Fiber (GI-POF) for low cost and improved data rate RoF transmission. The performance of the proposed system is assessed by comparing power penalties at FEC limit (3.8×10^{-3}) of BER while employing no optical fiber effects, which is considered as benchmark, with 200 meter and 400 meter fiber lengths. The novelties of this paper are summarised as follows:

- We design and analyze the performance of 60 GHz mm-wave enabled full-duplex PAM-4 based MIMO signal transmission over 400 meter Multimode Plastic Optical Fiber (MM-POF). We show that the proposed architecture is capable of achieving data rate of 16×12 Gbps for the PAM-4 data stream.
- We also show that the receiver sensitivities of the received PAM-4 signals at FEC limit of 3.8×10^{-3} of BER are achieved at -8.81 dBm (LP01) and -6.1 dBm (LP11) for DL while at -7.5 dBm (LP01) and -4.9 dBm (LP11) for UL in B2B system. These values are considered as reference for 200 meter and 400 meter length of fiber. Least Mean Square (LMS) equalization is performed to mitigate the channel effects and the power penalties for all channels at 200 meter and 400 meter fiber lengths are achieved below 1.5 dBm.
- Additionally, we show that polarization states of coherent LP01 and LP11 modes can be generated for each sideband of the multi-wavelength comb from a single laser and RF source, in order to attain a 16×16 MIMO transmission at the RAU.

The proposed system is designed to increase the access network capacity and to increase the attainable number of supported users, and hence it is desirable to exploit the benefits of MMF by utilizing its modes as independent channels. Meanwhile, the cost of the design can be minimized by using POF and multi-wavelength generator, as in the proposed design. This is a proof of concept towards next generation communication on the lines of the BlueSpace Project[26]. Commercially available software OptiSystem is used to perform simulation study of the proposed model. It is noteworthy that in the proposed architecture, off-the-shelf optical components are employed in the design to reduce the cost and engineering complexity. The signal generation and transmission techniques do not require application of complex signal processing. However, off-line Digital Signal Processing (DSP) is applied on the received PAM-4 signal for further processing as detailed in Section 3.

The rest of the paper is organised as follows. In Section 2, DAS-RoF architecture is discussed in detail. This section presents the design and working for DL transmission, RAU and UL transmission. Finally, in Section 3 the results are discussed and conclusions drawn from this work are presented in Section 4.

2 | THE PROPOSED DAS-ROF ARCHITECTURE

To facilitate a large number of users in dense areas such as in football stadiums or concert halls, there is a need of an RoF link capable of supporting very high data rate, low latency and higher bandwidth. RoF system is composed of a CU and multiple RAUs. Each RAU is connected to the CU via optical fiber link. All signal processing, wavelength management and modulation are performed at the CU[35], whereas the role of RAU is simply to convert optical signal to electrical form and perform amplification and transmission of the wireless signal at a designated frequency and thus making the RAU simple and inexpensive. The higher capacity RoF link is proposed for the scenario shown in Figure 1. This scenario is based upon the star topology where multiple RAUs are directly connected with a CU in a densely populated stadium, as shown in Figure 1. SDM along with PDM is used to solve the capacity issues in the fronthaul network by employing MIMO and 60 GHz mm-wave frequency is used to support ultra-high data rates at RAUs.

RoF technology is suitable for DAS network, where multiple small cells are employed to enhance the coverage and data rate by using frequency reuse. Furthermore, mm-wave has an intrinsic property that it can be utilized for short range radio transmission which will reduce the inter-cell interference among small cells[36]. The traditional way of generating mm-wave signals is by

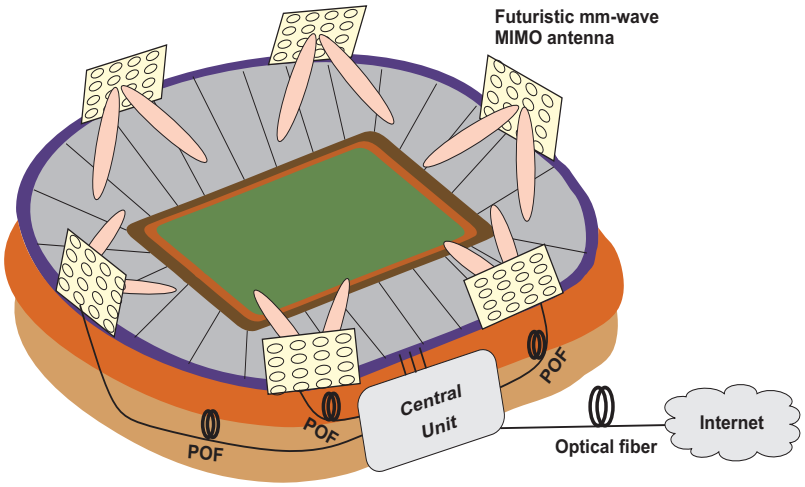

FIGURE 1 MIMO enabled mm-wave RoF link for star architecture.

using high radio frequency mixers, which tend to degrade the performance[37]. This problem can be solved by generating mm-wave by employing remote heterodyne detection at the RAU. In the proposed architecture mm-wave signals are generated at the RAU by using all optical processing. In Figure 2, the detailed Physical layer design is presented for the proposed architecture. It consists of CU and RAU blocks, where the CU is responsible for multi-wavelength generation and DL data transmission, while the RAU is reserved for DL data reception, generation of mm-wave signals and UL data transmission. The configuration setup for multi-wavelength generator can be seen at the bottom left side in Figure 2. It consists of a CW laser source, a sinusoidal RF source and a DD-MZM. The chirping phenomenon of MZM plays a vital role in multiple optical carriers' generation, where the term chirping refers to the change in the phase of optical signal with time at the output of a phase modulator. This chirping effect is boosted in our case to generate the desired number of optical carriers. The desired chirp is achieved by controlling the electrical driving signals applied to the upper and lower arms of the DD-MZM, separately. As a result, the optical signals experience change in phase after passing through DD-MZM[38] and then the obtained optical signals at the output of DD-MZM are combined to generate the desired multiple coherent optical carriers. A sinusoidal RF signal is modulated with CW laser source's output by using a DD-MZM as it may be observed from Figure 2. The optical field emitting from CW laser source is the input to DD-MZM and is given as follows:

$$\xi_{\mathrm{i}}(t) = \sqrt{\rho_{\mathrm{o}}}\exp(j2\pi f_{\mathrm{o}}t), \tag{1}$$

where, f_{o} and ρ_{o} are frequency and power of the optical carrier, respectively. The output of DD-MZM, modulated optical field, can be written as follows[39,40]:

$$\xi_{\mathrm{o}}(t) = \frac{\xi_{\mathrm{i}}(t)}{2}\left[\exp\left\{j\frac{(1+\gamma)\pi V_1(t)}{V_\pi}\right\} + \exp\left\{j\frac{(1-\gamma)\pi V_2(t)}{V_\pi}\right\}\right]. \tag{2}$$

In the above equation $V_1(t)$ and $V_2(t)$ are the applied driving electrical voltages to the upper and lower branches of DD-MZM, respectively. V_π is the voltage required to induce a phase shift of 180^{o} in optical signals and γ is the chirp factor. We are operating the DD-MZM in push-pull mode in order to obtain multiple sidebands. To operate MZM in push-pull mode, the applied voltages of RF signals are chosen such that $V_2(t) = -V_1(t)$. **The applied RF signal can be written as**

$$V_1(t) = \frac{1}{2}\left\{\upsilon_{\mathrm{rf}}\sin(\omega_{\mathrm{rf}}t) + \upsilon_{\mathrm{DC}}\right\}, \tag{3}$$

where υ_{rf} is the amplitude of the RF signal, υ_{DC} is the DC bias voltage and ω_{rf} is the angular frequency of the RF signal. Here, $\omega_{\mathrm{rf}} = 2\pi f_{\mathrm{rf}}$ and f_{rf} is the frequency of the sinusoidal RF signal. After substituting Equation (3) into Equation (2), we get the following expression

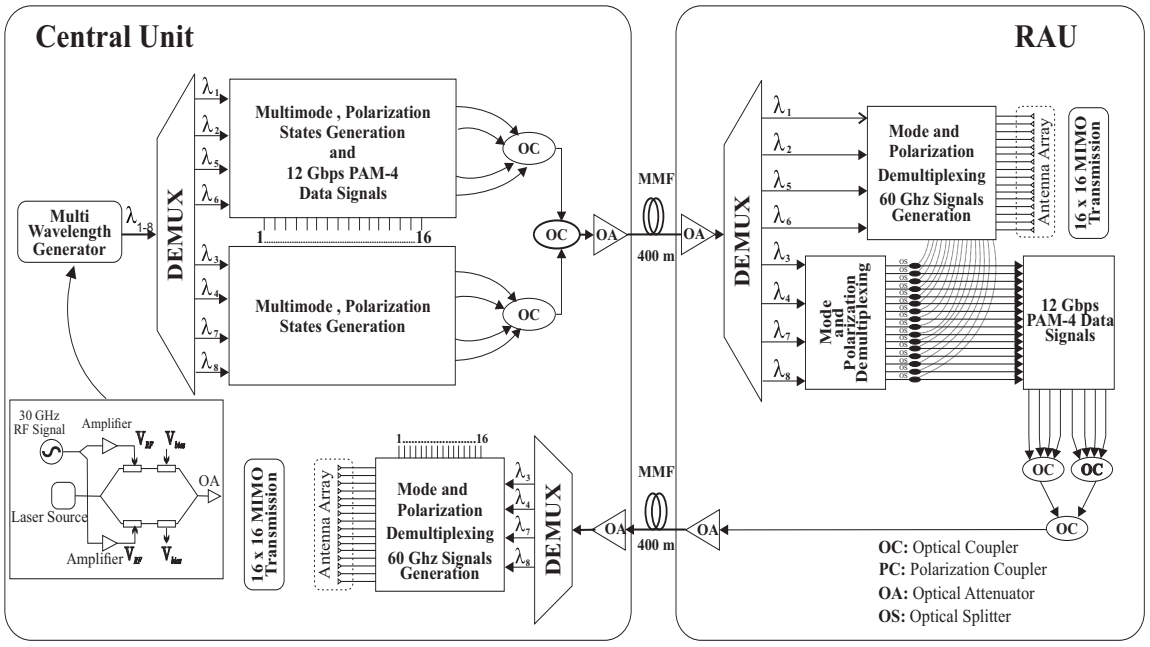

FIGURE 2 Schematic of proposed PAM-4 based mm-wave enabled 16 × 16 MIMO RoF architecture. OS:Optical Splitter, OC: Optical Coupler, EA: Electrical Amplifier.

$$\xi_{\mathrm{o}}(t) = \frac{\xi_{\mathrm{i}}(t)}{2}\left[\exp\left\{j\frac{(1+\gamma)\pi(v_{\mathrm{rf}}\sin(\omega_{\mathrm{rf}}t)+v_{\mathrm{DC}})}{2V_{\pi}}\right\} + \exp\left\{-j\frac{(1-\gamma)\pi(v_{\mathrm{rf}}\sin(\omega_{\mathrm{rf}}t)+v_{\mathrm{DC}})}{2V_{\pi}}\right\}\right]. \tag{4}$$

$$\xi_{\mathrm{o}}(t) = \frac{\xi_{\mathrm{i}}(t)}{2}\left[\exp\{j\zeta_2\sin(\omega_{\mathrm{rf}}t)\}\exp(j\zeta_1) + \exp\{-j\zeta_4\sin(\omega_{\mathrm{rf}}t)\}\exp(-j\zeta_3)\right]. \tag{5}$$

where

$$\zeta_1 = \frac{\pi(1+\gamma)}{2V_{\pi}}v_{\mathrm{DC}},$$

$$\zeta_2 = \frac{\pi(1+\gamma)}{2V_{\pi}}v_{\mathrm{rf}},$$

$$\zeta_3 = \frac{\pi(1-\gamma)}{2V_{\pi}}v_{\mathrm{DC}}, \tag{6}$$

$$\zeta_4 = \frac{\pi(1-\gamma)}{2V_{\pi}}v_{\mathrm{rf}}.$$

The DD-MZM, in this case, is operating at the quadrature point to achieve intensity modulation. In this mode the variation of the applied RF signal occur around the operating point of DD-MZM which causes no distortion in complete

swings of applied RF signal. For this configuration, DC bias voltage is set equal to $V_\pi/2$, peak to peak modulation voltage is set equal to V_π and the peak voltage of RF signal $\upsilon_{\mathbf{rf}}$ is set equal to $V_\pi/2$. Therefore, by putting $\upsilon_{\mathbf{rf}} = \upsilon_{\mathbf{DC}} = V_\pi/2$ in Equation (6), we get $\zeta_1 = \zeta_2$ and $\zeta_3 = \zeta_4 = \pi/2 - \zeta_1$.

After putting ζ_2, ζ_3 and ζ_4 in terms of ζ_1 in Equation (5), the following equation is obtained

$$\xi_o(t) = \frac{\xi_i(t)}{2}\exp(j\zeta_1)\Bigg[\exp\{j\zeta_1\sin(\omega_{rf}t)\} - j\exp\left\{(-j(\frac{\pi}{2}-\zeta_1)\sin(\omega_{rf}t))\right\}\Bigg]. \tag{7}$$

Finally, the output of DD-MZM in Equation (7) can be written as[41]

$$\xi_o(t) = \frac{\sqrt{\rho_o}\exp(j\zeta_1)}{2}\Bigg[\left\{J_o(\zeta_1) - jJ_o(\zeta_1 - \frac{\pi}{2})\right\}\exp(j2\pi f_o t) + \sum_{n=-\infty}^{\infty} J_n(\zeta_1)\exp(j2\pi(f_o + nf_{rf})t) - j\sum_{n=-\infty}^{\infty} J_n(\zeta 1 - \frac{\pi}{2})\exp(j2\pi(f_o + nf_{rf})t)\Bigg]. \tag{8}$$

where $J_o(\zeta_1)$ and $J_n(\zeta_1)$ represent the Bessel function of center frequency (f_o) and n^{th}-order, respectively. Here, n is the number of generated side-bands. From Equation (8), it can be clearly seen that at a given f_{rf} the number of generated side-bands is proportional to ζ_1. This ultimately shows the dependence of the number of side-bands on the chirp factor γ for fixed values of υ_{rf} and υ_{DC}. The frequency (f_{rf}) of the RF signal controls the spacing between the generated side-bands.

Each side band is equally spaced at 30 GHz from the center frequency of the CW laser, as it can be clearly seen in Figure 3. Power fluctuation of all generated side bands is less than 5dB, as shown in Figure 3. Therefore, any side band can be used as an optical carrier for data transmission. Optical carriers λ_1, λ_2, λ_3, λ_4, λ_5, λ_6, λ_7 and λ_8 are shown in inset of Figure 3 with power fluctuation among them being less than 5 dB. Eight wavelengths have been chosen to achieve 16×16 optical MIMO transmission. These optical carriers are selected as a design example, while any generated optical carrier can be used for transmission. On the other hand, while choosing carriers for Downlink (DL) and Uplink (UL), care has been taken so that frequency difference between DL optical carriers and UL optical carriers should be 60 GHz because it will be used for heterodyne detection at the reciever to generate 60 GHz mm-wave. Therefore, for DL transmission we have used λ_1, λ_2 and λ_5, λ_6 while for UL transmission λ_3, λ_4 and λ_7, λ_8 are used, respectively as shown in Figure 2.

Furthermore, to achieve 16×16 MIMO, thirty-two channels at CU need to be generated for both DL and UL. To generate thirty-two channels, Linearly Polarized (LP) modes of MM-POF are exploited to realize optical MIMO transmission by employing MDM in the MM-POF. The theoretical principle of optical MIMO transmission is based on the propagation of modes in the MMF having similar phase constants and group delays. These modes can be placed together in a group set and this arrangement is referred to as Principal Mode Group (PMG) represented by M[42]. Furthermore, these modes are known as Linearly Polarized (LP_{lm}) modes for the weakly guiding assumption ($n_1 \approx n_2$) of optical fiber where n_1 and n_2 are the refractive indexes of core and cladding of the MM-POF, respectively. The subscripts l and m represents radial and azimuthal mode numbers, respectively. PMG expression is given below[43]:

$$M_{PMG} = l + 2m + 1. \tag{9}$$

M_{PMG} is 3 and 4 for LP01 and LP11 modes, respectively. The transmission bandwidth is enhanced when PMG is utilized as independent channels instead of individual mode in optical fiber[43]. This facilitates the optical MIMO transmission by employing MGDM in the MMF. Based on this theory, 16×16 optical MIMO transmission are achieved in the proposed architecture. Each wavelength, for example λ_1, is first passed through the mode generator to generate LP01 and LP11 modes which is then passed through polarization splitter (PS), as shown in Figure 4, to generate orthogonal x-polarization (X-POL) and y-polarization (Y-POL) channels. This results in the generation of four independent channels from λ_1. Similarly, for eight wavelength (λ_1-λ_8), total thirty two ($8\lambda s \times 2$ LP modes $\times$ 2 polarizations) independent channels will be available for DL and UL transmission. Four

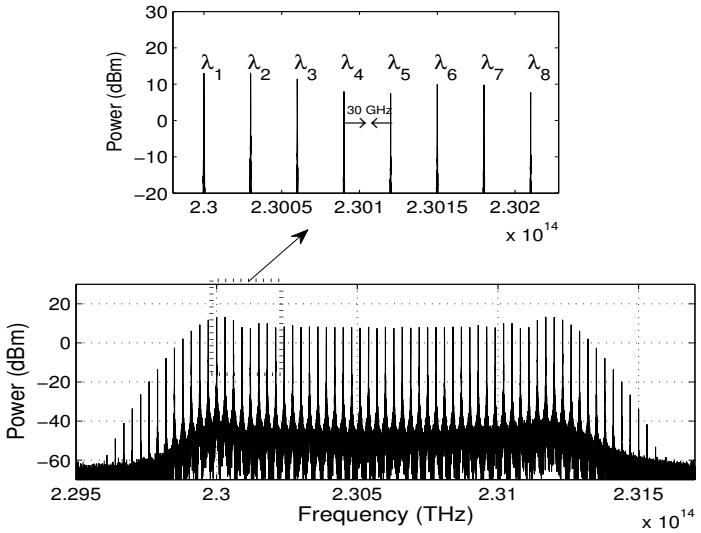

FIGURE 3 Multi-wavelength comb spectrum.

TABLE 1 Parameters of POF used for simulation.

Parameter	Value
Numerical Aperture	0.185 ± 0.015
Length	0.4 (km)
Core radius	50 ± 5 (μm)
Dispersion slope	≤ 0.06 (ps/nm^2.km)
Over-cladding diameter	490 ± 5 (μm)
Attenuation	60 (dB/km)
Zero dispersion wavelength	1200 - 1600 (nm)

wavelengths λ_1, λ_2, λ_5, λ_6 are used for DL transmission and the remaining four wavelengths λ_3, λ_4, λ_7 and λ_8 are reserved for UL transmission.

2.1 | Downlink Transmission

Optical signal at the output of DD-MM is fed into 1×8 demultiplexer (DEMUX) as shown in Figure 2, where each channel of 30 GHz spacing have Gaussian filter properties with 3 dB bandwidth of 20 GHz. Each wavelength at the output of the DEMUX is used to generate LP modes, LP01 and LP11, by using multimode generator (MMG) where each mode acts as a separate channel as shown in Figure 4. Furthermore, these LP modes are further passed through Polarization Splitter (PS) to generate orthogonal polarization states X-POL and Y-POL of each mode which can be clearly seen in Figure 4. These polarization states behave as independent channels and are used to modulate the PAM-4 signal by using Single Drive Mach-Zehnder Modulator (SD-MZM), as shown in Figure 4. Polarization states of wavelengths λ_1, λ_2 and λ_5, λ_6 are modulated with PAM-4 signal of data rate 12 Gbps, as shown in Figure 4. In a similar manner, the remaining four wavelengths λ_3, λ_4 and λ_7, λ_8 form sixteen independent unmodulated channels as depicted in Figure 2, which are then used for UL transmission as will be discussed later. Polarization states are combined by using Polarization Combiner (PC). The modulated polarization composite signals λ_1, λ_2, λ_5 and λ_6 and unmodulated signals λ_3, λ_4, λ_7 and λ_8 are coupled by using an Optical Coupler (OC) and transmitted through 400m PF-GI-POF (Fiberoptics Giga-POF-50SR)[44]. The typical Parameters of commercially available POF called Fiberoptics Giga-POF-50SR are given in Table 1. These values of the parameters are used in this simulation.

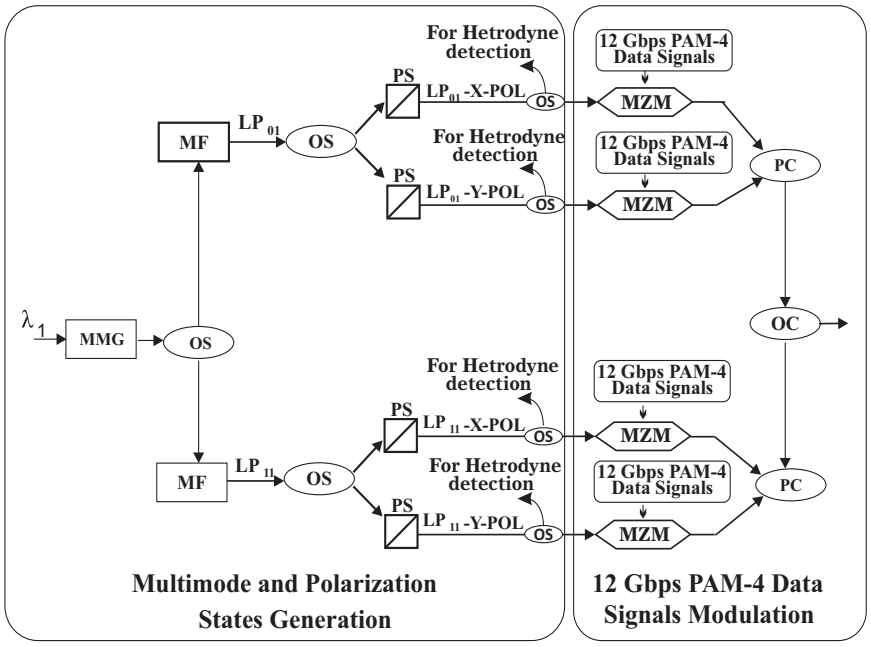

FIGURE 4 Design of DL Transmission; MMG: MultiMode Generator; MF: Mode Filter; PS: Polarization Splitter; PC: Polarization Coupler; MZM: Mach-Zehnder Modulator; OC: Optical Coupler; OS: Optical Splitter.

2.2 | Remote Antenna Unit

At the optical receiver, after amplifying the received signal it is fed into the demultiplexer which separates all wavelengths as shown in Figure 2. After the separation, each wavelength is further passed through mode filters to filter out LP01 and LP11 as presented in Figure 5. LP modes of λ_1- λ_8 are then passed through PS to separate each orthogonal polarization state of LP modes, as shown in Figure 5. These X-POL and Y-POL states of LP01 and LP11 modes of wavelengths λ_1, λ_2, λ_5, λ_6 contain the data to be transmitted wirelessly by using mm-wave frequency.

60 GHz millimeter-wave frequency used in the proposed system is one of the listed viable frequencies (24 GHz to 86 GHz) proposed for 5G by the International Telecommunication Union (ITU)[45,46]. However, the system described in this manuscript is flexible and can be modified to achieve desired millimeter wave frequency by controlling the frequency of the RF source. To generate mm-wave at the RAU two optical signals of frequency difference 60 GHz are required for heterodyne detection[47]. Therefore, after demultiplexing, LP01 and LP11 modes of each wavelength are achieved by using mode filter, LP01 mode of λ_1 is passed through PS to get X-POL and Y-POL, as shown in Figure 5. X-POL of LP01 of λ_1 is coupled with X-POL of LP01 mode of λ_3 as presented in Figure 5 which results in a frequency difference of 60 GHz, which can be clearly seen in Figure 3. This coupled signal is fed into photodiode, which generates an electrical signal of 60 GHz frequency. As shown in Figure 5, the electrical signal is then passed though an electrical band pass filter (BPF) which has a center frequency at 60 GHz. Similarly, mm-wave signal is generated for the rest of the antenna elements of 16 antenna array. The beating of each data modulated signal with unmodulated signal to generate mm-wave signals is shown in Table 2. Then, 60 GHz signal at the output of the BPF is fed into the antenna for wireless transmission.

At the receiver side, the 60 GHz signal is split into two parts by using a splitter which is then down-converted using the self mixing technique[48]. As stated in[48] two copies of high frequency signals can be mixed together to generate a low frequency signal without using a separate oscillator. To retrieve the baseband signal, the down converted signal is passed through Low Pass Filter (LPF). Further equalization is performed at the receiver side to mitigate the channel effects. The received signal is normalized and resampled at two samples per symbol. For equalization, LMS algorithm is used with the aid of training symbols which is helpful for initial taps convergence. Once taps are converged, LMS switches to the decision directed mode. Finally, BER is calculated after hard decision by employing error counting method.

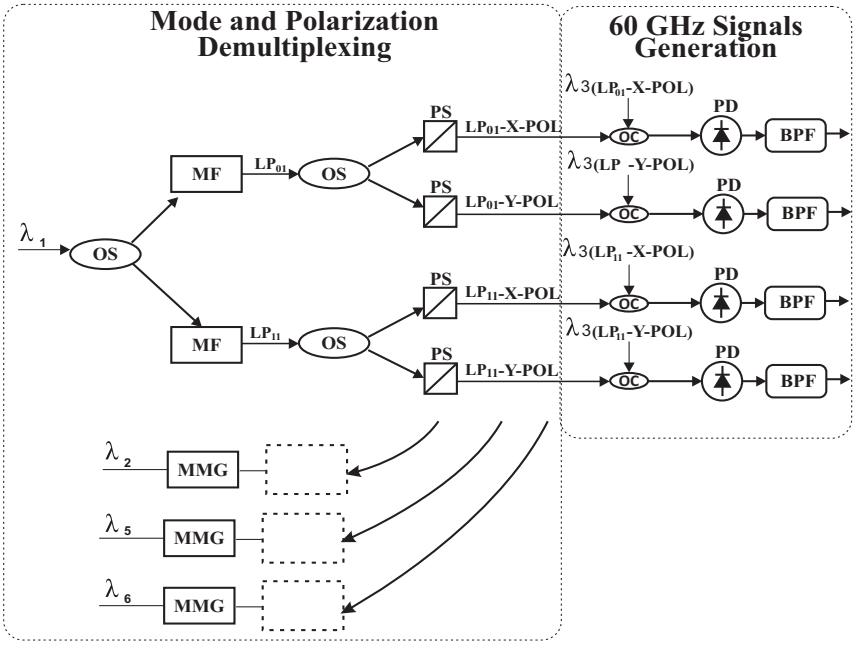

FIGURE 5 Remote Antenna Unit (RAU); PD: Photo Detector; BPF: Bandpass Filter; OS: Optical Splitter; MF: Mode Filter; OC: Optical Coupler.

TABLE 2 Signal beating for mm-wave signal generation.

LP01	LP11
(λ_1-X-POL), (λ_3-X-POL)	(λ_1-X-POL), (λ_3-X-POL)
(λ_2-X-POL), (λ_4-X-POL)	(λ_2-X-POL), (λ_4-X-POL)
(λ_5-X-POL), (λ_7-X-POL)	(λ_5-X-POL), (λ_7-X-POL)
(λ_6-X-POL), (λ_8-X-POL)	(λ_6-X-POL), (λ_8-X-POL)
(λ_1-Y-POL), (λ_3-Y-POL)	(λ_1-Y-POL), (λ_3-Y-POL)
(λ_2-Y-POL), (λ_4-Y-POL)	(λ_2-Y-POL), (λ_4-Y-POL)
(λ_5-Y-POL), (λ_7-Y-POL)	(λ_5-Y-POL), (λ_7-Y-POL)
(λ_6-Y-POL), (λ_8-Y-POL)	(λ_6-Y-POL), (λ_8-Y-POL)

2.3 | Uplink Transmission

The Unmodulated sixteen channels (4λs × 2 LP modes × 2 polarizations) of the wavelengths λ_3, λ_4, λ_7 and λ_8, mentioned in Section 2.1. A are reserved for UL transmission. They are used to modulate with a PAM-4 data stream similar to the procedure adopted for λ_1 in DL transmission, as shown in Figure 4. Polarization states of all LP01 and LP11 modes of wavelength λ_3, λ_4, λ_7 and λ_8 are combined by the PC and then the optical channels are coupled by using the OC. This multiplexed signal is transmitted to the CU through 400 m PF-GI-POF. The received signal at the CU is passed through a similar process as discussed for the RAU. However, the generation of 60 GHz mm-wave signal is possible only when two wavelengths having frequency difference of 60 GHz are available. Hence, the wavelengths, which are combined to generate 60 GHz mm-wave frequency, are selected at the CU for heterodyne detection, as shown in Figure 2. The optical signals, which are combined to perform heterodyne detection for UL transmission, are shown in Table 2.

2.4 | Complexity Analysis

The computational complexity of the applied DSP for PAM-4 is analysed in the proposed system as follows. The functions, such as LMS based equalizer, which have higher complexity are only considered for computational complexity and less complex and simple functions are ignored. The LMS based equalizer can be implemented in both frequency or time domain namely as Frequency Domain Equalizer (FDE) and Time Domain Equalizer (TDE), respectively[49]. However, it is familiar that the FDE is less complex and simple to implement than TDE[50]. Therefore, we have considered FDE for equalization having tap length of N. It may be noted that for implementation of DSP in ASIC, the multiplier's cost is comparatively higher than an adder[51]. Considering this fact only, the real number of multipliers are estimated to calculate the computational complexity of the applied DSP. To obtain $N/2$ symbols at the output of the equalizer, overlap-save method[52] with 50 percent overlap is considered for the implementation of FDE whereas for output calculation of one block, N multiplications will be required and then N multiplication will be required for updating the taps. Similarly, $4Nlog_2(N)$ multipliers are used for 8 Fast Fourier Transform/Inverse Fast Fourier Transform (FFT/IFFT) process (inputs: 2 FFT, output: 1 FFT, error calculation: 1 FFT and gradient constraint employment: 4 FFT). Classical radix-2 algorithm[53] is used for the FFT implementation which requires $Nlog_2(N)/2$ multipliers for the execution of the FFT of order N. Based on the above calculations, the expression for the computational complexity, C, for PAM-4 is given below.

$$C = [4 + 10log_2(N)]/[log_2(M)] \tag{10}$$

Where M is the number of levels of PAM-M signal, which is 4 for PAM-4. Hence, for the system employing PAM-4 and using 21-tap equaliser, the computational complexity is 24 real multiplications per bit.

3 | RESULTS AND DISCUSSIONS

To evaluate the system performance, BER is used as a performance metric to validate the proposed architecture. The DSP techniques are employed on the received PAM-4 signal to combat the channel effects. The flow chart of the applied DSP is shown in Figure 6 and explained as follows. The received signal is resampled at two samples per symbol after normalization[54]. Then, the LMS algorithm is used for equalisation with the aid of training symbols, which is helpful for initial taps convergence. Once taps converge, the LMS switches to the decision directed mode. Finally, the BER is evaluated, after hard decision by employing error counting method. **Eye diagrams and their corresponding Probability Density Functions (PDFs) for both LP01 and LP11 modes at received optical powers of -8.81 dBm and -6.1 dBm are shown in Figures 7a, 8a and Figures 7b, 8b respectively, for DL transmission. These readings are taken at the BER of 3.8×10^{-3}, which is defined as the Forward Error Correction (FEC) limit[22]. It is clear from Figure 7a and 8a that the eye opening is quite reasonable at the mentioned FEC limit.**

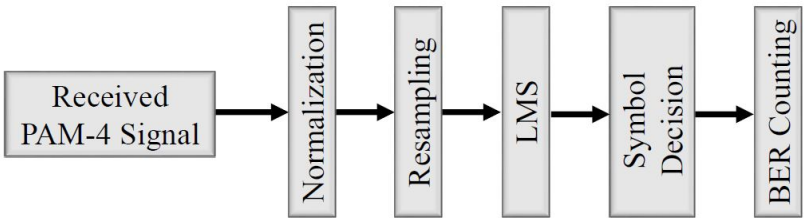

FIGURE 6 Flow chart of off-line DSP.

To evaluate the system performance, BER of each channel is calculated for different fiber lengths such as Back to Back (B2B), 200 meters and 400 meters. First, BER for B2B system is calculated for which the effects of fiber are ignored and then this BER curve is considered as a benchmark for the fiber lengths of 200 meters and 400 meters. Our proposed architecture is suitable for implementation in an indoor environment such as an office, airport or similar commercial buildings. In such places, the distances involved are smaller and it is desirable to increase the coverage and capacity of the network. Due to the high attenuation of the POF, the maximum possible length of fiber for the proposed architecture at 12 Gbps is 400 meters. The power of the received signal is attenuated with an optical attenuator and the received power is measured with the help of a power

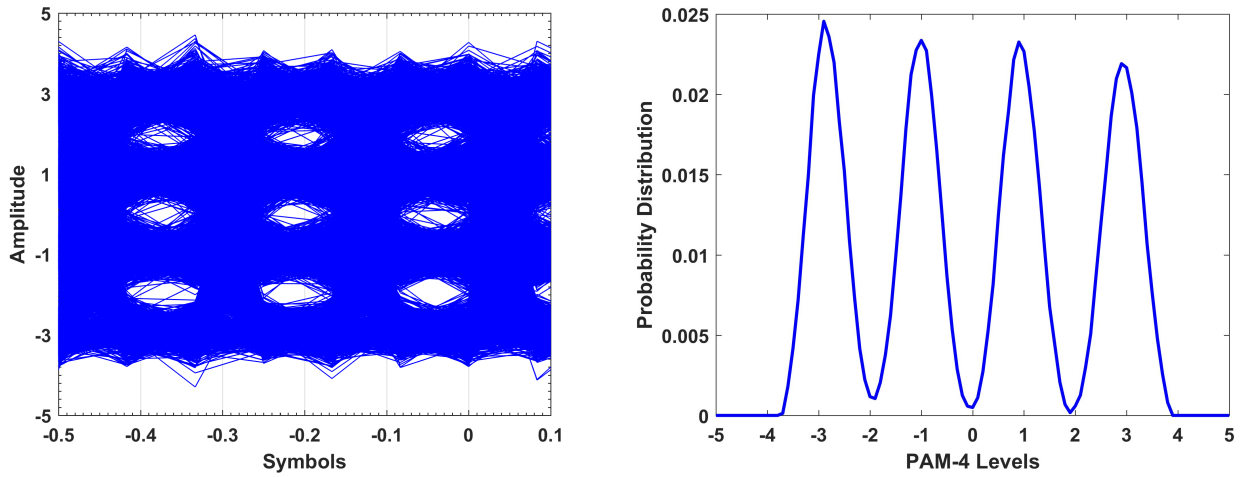

(a) (b)

FIGURE 7 Performance of $LP01_{x\text{-}pol}$ mode for DL transmission at −8.81 dBm ROP after equalization (a) Eye diagram (b) Probability Density Function.

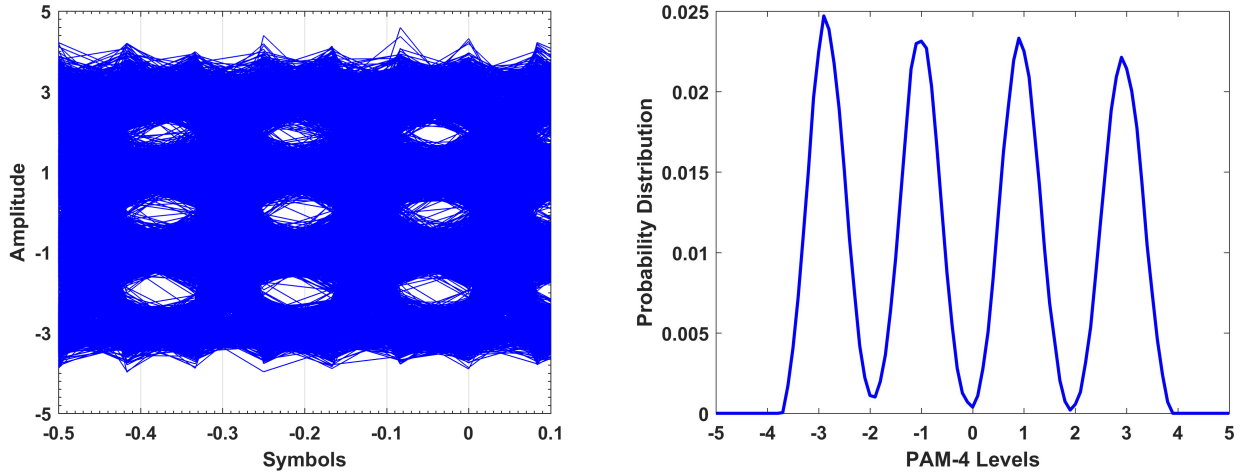

(a) (b)

FIGURE 8 Performance of $LP11_{x\text{-}pol}$ mode for DL transmission at −6.1 dBm ROP after equalization (a) Eye diagram (b) Probability Density Function.

meter. BER is calculated with respect to the Received Optical Power (ROP) as shown in Figure 11 and Figure 12 for DL and UL transmission, respectively. The BER for the DL transmission can be seen in Figure 11 for both LP01 and LP11 modes at B2B, 200 meters and 400 meters. It can be clearly seen that the receiver sensitivity for the LP01 is less than that of the LP11 at the FEC limit. The receiver sensitivity at FEC limit for LP01 mode is achieved at −8.81 dBm, while for LP11 mode it is achieved at −6.1 dBm for B2B transmission and is considered as benchmark for 200 meters and 400 meters transmission lengths of optical fiber. It may be noted that for B2B transmission no optical fiber is used and there is no chirp on the optical signal caused by the optical fiber at PD. The reasons for this degraded performance for LP11 mode as compared to LP01 mode could be the mode coupling loss in MMF and the occurrence of inter modal cross talk. As discussed in[55,44], inter modal coupling may be ignored for short range optical communication links. In addition, it has been explained in[56] that output polarization states of either modes are not affected in the absence of mode coupling. It is worth noting that the proposed model is designed for

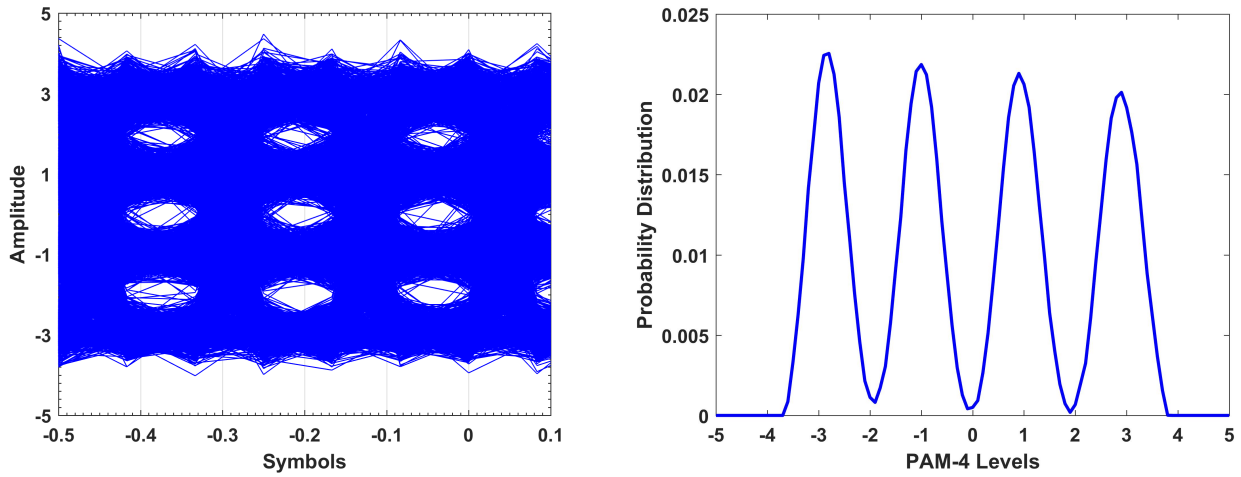

(a) (b)

FIGURE 9 Performance of $LP01_{x\text{-}pol}$ mode for UL transmission at −7.5 dBm ROP after equalization (a) Eye diagram (b) Probability Density Function.

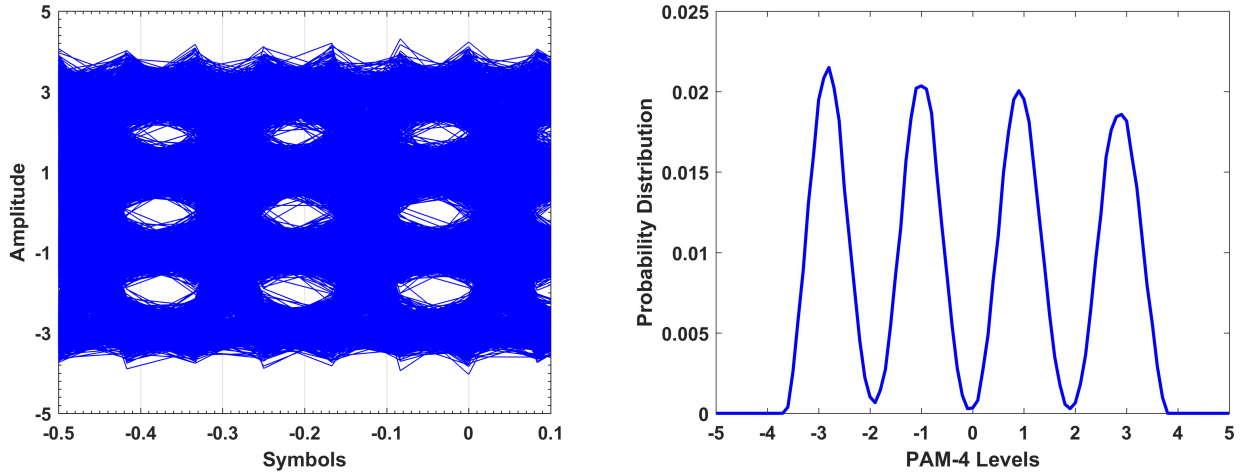

(a) (b)

FIGURE 10 Performance of $LP11_{x\text{-}pol}$ mode for UL at −4.9 dBm after equalization (a) Eye diagram (b) Probability Density Function.

short range communication and as reported in[55] and[56], inter-modal coupling and polarization coupling do not affect short range communication significantly. However, the degraded performance of LP11 mode is due to incompatibility between the detection area of the photodetector and the higher order LP11 mode[57]. To overcome this performance difference between fundamental mode LP01 and higher order mode LP11, photodetectors need to be designed which support higher order mode LP11 along with the fundamental mode LP01. The power penalties with respect to B2B for 200 meters and 400 meters lengths are 0.6 dBm and 1.4 dBm, respectively, which can be clearly seen in Figure 11.

Similarly, to evaluate UL transmission, the BER is calculated for the received signal after low pass filtering at the receiver sensitivity for BER of 3.8×10^{-3}. A similar DSP technique has been applied as discussed for DL transmission to calculate the BER. **Clear eye diagram and PDFs for LP01 and LP11 of received PAM-4 signal after equalization with received optical powers of −7.5 dBm and −4.9 dBm are shown in Figure 9 and Figure 10, respectively, for UL transmission.** It can be

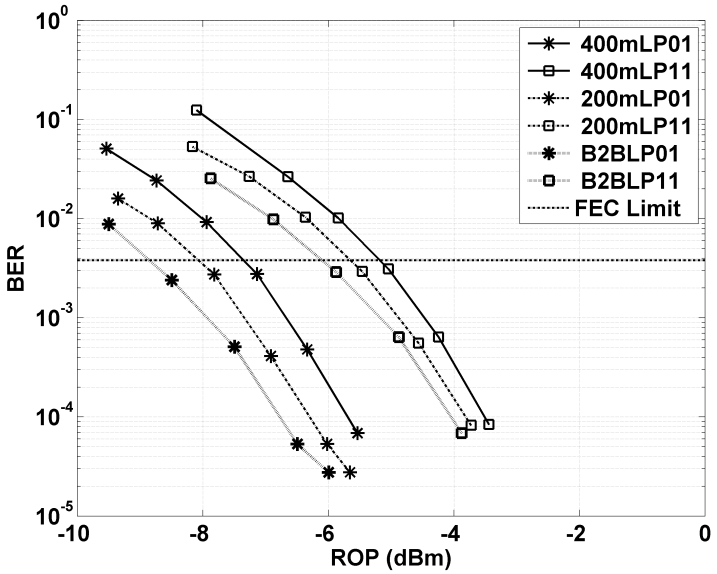

FIGURE 11 BER versus ROP at B2B, 200 meter and 400 meter length of POF for DL transmission.

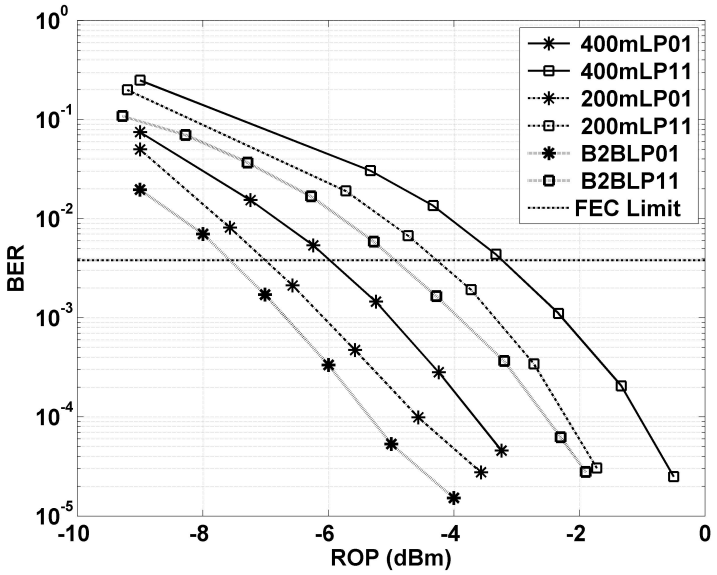

FIGURE 12 BER versus ROP at B2B, 200 meter and 400 meter length of POF for UL transmission.

seen that BER is degraded as compared to DL as presented in Figure 12 in which receiver sensitivity for LP01 mode and LP11 mode is achieved approximately at −7.5 dBm and −4.9 dBm, respectively, for the case of B2B transmission. This degraded performance is due to the fact that the optical carriers travel all the way from CU to RAU and back from RAU to CU. Figure 12 shows the power penalties with respect to B2B for 200 meters and 400 meters UL transmission length and are observed approximately 0.5 dBm and 1.5 dBm, respectively.

It can be inferred from the results achieved that the generated multiple wavelengths can be used to employ PDM along with MDM to enhance the capacity of a WDM-RoF link. To achieve acceptable BER of the proposed model, the lengths of MMF and data rate are adjusted accordingly. All of the parameters used in our simulations are in accordance with commercially available components. The summary of the related work discussed in Section 1 is presented in Table 3. The important features

Table 3. Comparison with current state-of-the-art approaches.

Author/Year	Multi-wavelength Comb	Duplex	MM-POF	MDM-PDM-WDM	mm-wave	MIMO	Data Rate
Zhong et al.[14]/2015	×	×	×	×	×	×	112 Gbps
Wang et al.[17]/2017	×	×	×	×	✓	×	8.4 Gbps
Shao et al.[21]/2017	✓	✓	×	×	×	×	10 Gbps
Zhou et al.[19]/2018	×	×	×	×	✓	×	20 Gbps
Zhou et al.[20]/2018	×	×	×	×	✓	×	13 Gbps
Deng et al.[18]/2018	×	×	×	×	✓	×	4.63 Gbps
Raza et al.[44]/2018	×	✓	300 meter	×	✓	2×2	2 Gbps
Proposed Work	✓	✓	400 meter	✓	✓	16×16	16×12 Gbps

linked with RoF architectures are highlighted in Table 3 in the first row. The state-of-the-art RoF architectures proposed by researchers [14,17,21,18,19,20,44], as discussed in Section 1, are enlisted in Table 3. Against this background, the shortcomings in these studies have been addressed and an architecture having maximum features is employed in the proposed scheme to achieve high data rate at low cost. It is clear from Table 3 that data rates of 16×12 Gbps is achieved at 400 meter length of MM-POF. In addition, the proposed model is designed to support 16×16 MIMO transmission for short range mm-wave enabled RoF Communication.

4 | CONCLUSIONS

In this paper, we have proposed a 16×16 MIMO enabled full duplex RoF architecture, where the proposed architecture demonstrated full duplex 16×16 MIMO spatial channels each carrying 12 Gbps for DL and UL and an overall data rate of 16×12 Gbps has been achieved. MDM along with PDM multiplexing techniques have been used to enhance the data rate. Furthermore, mm-wave of 60 GHz is generated at the RAU by utilising the principle of heterodyne detection. Offline DSP is employed and LMS algorithm is used as an equalizer to recover PAM-4 signal at the receiver. To make the proposed architecture cost efficient, a single laser source based on multiple optical carriers and POF is employed. BER at the FEC limit for both DL and UL transmission have been achieved for different length of fiber at reasonable ROP values. The proposed architecture can further be extended to realise massive MIMO.

References

1. Cisco Public, "Cisco Visual Networking Index: Global Mobile Data Traffic Forecast Update, 2016 - 2021", Cisco White Paper, March 2017.

2. Larsson EG, Edfors O, Tufvesson F, Marzetta TL. Massive MIMO for next generation wireless systems. *IEEE Communications Magazine* 2014; 52(2): 186-195. doi: 10.1109/MCOM.2014.6736761

3. Thomas VA, El-Hajjar M, Hanzo L. Millimeter-Wave Radio Over Fiber Optical Upconversion Techniques Relying on Link Nonlinearity. *IEEE Communications Surveys Tutorials* 2016; 18(1): 29-53. doi: 10.1109/COMST.2015.2409154

4. Sung M, Kim J, Kim E, et al. Demonstration of 5G Trial Service in 28 GHz Millimeter Wave using IFoF-Based Analog Distributed Antenna System. In: Optical Fiber Communications Conference and Exhibition (OFC); 2019: 1-3.

5. Thomas VA, El-Hajjar M, Hanzo L. Performance Improvement and Cost Reduction Techniques for Radio Over Fiber Communications. *IEEE Communications Surveys Tutorials* 2015; 17(2): 627-670. doi: 10.1109/COMST.2015.2394911

6. Ali B, Zamir N, Ng SX, Butt MFU. Distributed Matching Algorithms for Spectrum Access: A Comparative Study and Further Enhancements. *KSII Transactions on Internet and Information Systems* 2018; 12(4): 1594-1617.

7. Gilan MS, Yavarimanesh M, Mohammadi A. Cross-Layer Design Based on Adaptive Modulation and Queuing for AF Relay Selection System. *International Journal of Computer Networks and Wireless Communications (IJCNWC)* 2016; 6(6): 20-28.

8. Shirzadian Gilan M, Yavari Manesh M, Mohammadi A. Level Crossing Rate and Average Fade Duration of Amplify and Forward Relay Channels with Cochannel Interference. In: European Wireless 2016; 22th European Wireless Conference; 2016: 1-5.

9. Manesh MY, Olfat A. Sigmoid Function Detector in the Presence of Heavy-tailed Noise for Multiple Antenna Cognitive Radio Networks. In: 2017 IEEE International Conference on Communications (ICC); 2017: 1-5

10. Gilan MS, Manesh MY, Maham B. Optimized Target Packet Error Rate for a New Cross-layer Scheme in AF Relay Selection System. In: 2016 IEEE International Conference on Communication, Networks and Satellite (COMNETSAT); 2016: 1-6

11. Beas J, Castanon G, Aldaya I, Aragon-Zavala A, Campuzano G. Millimeter-Wave Frequency Radio over Fiber Systems: A Survey. *IEEE Communications Surveys Tutorials* 2013; 15(4): 1593-1619. doi: 10.1109/SURV.2013.013013.00135

12. Li X, Yu J, Xiao J, Chi N, Xu Y. W-Band PDM-QPSK Vector Signal Generation by MZM-Based Photonic Frequency Octupling and Precoding. *IEEE Photonics Journal* 2015; 7(4): 1-6. doi: 10.1109/JPHOT.2015.2449735

13. Li X, Yu J, Zhang J, et al. QAM Vector Signal Generation by Optical Carrier Suppression and Precoding Techniques. *IEEE Photonics Technology Letters* 2015; 27(18): 1977-1980. doi: 10.1109/LPT.2015.2448517

14. Zhong K, Zhou X, Gui T, et al. Experimental study of PAM-4, CAP-16, and DMT for 100 Gb/s Short Reach Optical Transmission Systems. *Opt. Express* 2015; 23(2): 1176–1189. doi: 10.1364/OE.23.001176

15. Ma J, Zhang J. Full duplex fiber link for alternative wired and wireless access based on SSB optical millimeter-wave with 4-PAM signal. *Optics Communications* 2015; 338: 578 - 584. doi: https://doi.org/10.1016/j.optcom.2014.11.039

16. Han L, Liang S, Xu J, Qiao L, Zhu H, Wang W. Simultaneous Wavelength- and Mode-Division (De)multiplexing for High-Capacity On-Chip Data Transmission Link. *IEEE Photonics Journal* 2016; 8(2): 1-10. doi: 10.1109/JPHOT.2016.2547419

17. Wang H, Zhou W, Yu J. PAM-4 signal delivery in one radio-over-fiber system. *Optical Engineering* 2017; 56: 56 - 56 - 5. doi: 10.1117/1.OE.56.10.106107

18. Deng R, Yu J, He J, Wei Y. Experimental demonstration of a real-time PAM-4 Q-band RoF system based on CMMA equalization and interleaved RS code. *Optical Fiber Technology* 2018; 42: 156 - 161. doi: https://doi.org/10.1016/j.yofte.2018.03.006

19. Zhou W, Zhang J, Han X, Kong M, Gou P. PAM-4 delivery based on pre-distortion and CMMA equalization in a ROF system at 40 GHz. *Optics Communications* 2018; 416: 61 - 65. doi: https://doi.org/10.1016/j.optcom.2018.01.067

20. Zhou W, Gou P, Wang K, et al. PAM-4 Wireless Transmission based on Look-up-table Pre-distortion and CMMA Equalization at V-band. In: Optical Fiber Communications Conference and Exposition (OFC); 2018: 1-3.

21. Shao Y, Chen F, Wang A, Luo Y, Chen L. Application research on 4-pulsed amplitude modulation in 10Gb/s passive optical access systems. *Optik* 2017; 146: 63 - 68. doi: https://doi.org/10.1016/j.ijleo.2017.08.072

22. Raza A, Zhong K, Ghafoor S, et al. SER estimation method for 56 GBaud PAM-4 transmission system. *Chin. Opt. Lett.* 2018; 16(4): 040604.

23. Chowdhury AM, Chien HC, Wei J, Chang GK. Multi-Service Multi-Carrier Broadband MIMO Distributed Antenna Systems for in-Building Optical Wireless Access. In: Optical Society of America; 2010: JWA57

24. Miyamoto K, Tashiro T, Higashino T, et al. Experimental demonstration of MIMO RF signal transmission in RoF-DAS over WDM-PON. In: International Topical Meeting on Microwave Photonics jointly held with the 2011 Asia-Pacific Microwave Photonics Conference; 2011: 25-28

25. Ravikanth J, Shah DD, Vijaya R, Singh BP, Shevgaonkar RK. Analysis of high-power EDFA operating in saturated regime at Îż=1530 nm and its performance evaluation in DWDM systems. *Microwave and Optical Technology Letters* 2002; 32(1): 64-70. doi: 10.1002/mop.10092

26. blueSPACE Information Leaflet, blueSPACE Consortium, Chesterfield, MO, USA, Ma. 2018.", [online]. Available: https://doi.org/10.5281/zenodo.1209373.

27. 5G-PHOS Video, 5G-PHOS Consortium, Thessaloniki, Greece, Nov. 2018. [Online]. Available: http://bit.ly/5GPHOSVideo.

28. Metro-Haul Consortium. (2017). Metro-Haul Project Introduction. [Online]. Available: https://metro-haul.eu/project.

29. Corral JL, Marti J, Fuster JM. General expressions for IM/DD dispersive analog optical links with external modulation or optical up-conversion in a Mach-Zehnder electrooptical modulator. *IEEE Transactions on Microwave Theory and Techniques* 2001; 49(10): 1968-1976. doi: 10.1109/22.954816

30. Park J, Sorin WV, Lau KY. Elimination of the fibre chromatic dispersion penalty on 1550 nm millimetre-wave optical transmission. *Electronics Letters* 1997; 33(6): 512-513. doi: 10.1049/el:19970325

31. Liu A, Wang X, Shao Q, Song T, Yin H, Zhao N. A low cost structure of radio-over-fiber system compatible with WDM-PON. In: Proceedings of 25th Wireless and Optical Communication Conference (WOCC); 2016: 1-3

32. Lim C, Yang Y, Nirmalathas A. Transport Schemes for Fiber-Wireless Technology: Transmission Performance and Energy Efficiency. *Photonics* 2014; 1: 67–83. doi: 10.1109/ACCESS.2016.2556011

33. Igweani UO, Al-Raweshidy HS. 60GHz delivery over SMF and MMF for in-door applications. In: Africon; 2013: 1-3

34. Thomas VA, El-Hajjar M, Hanzo L. Performance Improvement and Cost Reduction Techniques for Radio Over Fiber Communications. *IEEE Communications Surveys Tutorials* 2015; 17(2): 627-670. doi: 10.1109/COMST.2015.2394911

35. Gulistan A, Ghafoor S. Selfphase Modulation-based Multiple Carrier Generation for Radio Over Fiber Duplex Baseband Communication. *Photon Netw Commun* 2015; 29(2): 133-137.

36. Rappaport TS, Sun S, Mayzus R, et al. Millimeter Wave Mobile Communications for 5G Cellular: It Will Work!. *IEEE Access* 2013; 1: 335-349. doi: 10.1109/ACCESS.2013.2260813

37. Thomas VA, El-Hajjar M, Hanzo L. Millimeter-Wave Radio Over Fiber Optical Upconversion Techniques Relying on Link Nonlinearity. *IEEE Communications Surveys Tutorials* 2016; 18(1): 29-53. doi: 10.1109/COMST.2015.2409154

38. Zhang L, Song Y, Zou S, Li Y, Ye J, Lin R. Flat frequency comb generation based on Mach-Zehnder modulator and phase modulator. In: IEEE 12th International Conference on Communication Technology; 2010: 211-213

39. Koyama F, Iga K. Frequency chirping in external modulators. *Journal of Lightwave Technology* 1988; 6(1): 87-93. doi: 10.1109/50.3969

40. Ho KP, Kahn JM. Spectrum of externally modulated optical signals. *Journal of Lightwave Technology* 2004; 22(2): 658-663. doi: 10.1109/JLT.2004.824453

41. Korenev BG. *Bessel Functions and Their Applications*. CRC Press . 2002.

42. Olshansky, R. . Propagation in glass optical waveguides. *Rev. Mod. Phys.* 1979; 51: 341–367. doi: 10.1103/RevModPhys.51.341

43. Raddatz L, White IH, Cunningham DG, Nowell MC.

44. Raza A, Ghafoor S, Butt MFU. MIMO-enabled integrated MGDM-WDM distributed antenna system architecture based on plastic optical fibers for millimeter-wave communication. *Photonics network Communication* 2018; 35(2): 265-273.

45. ITU-T LIAISON STATEMENT 3GPP TSG SA4-S4-181152, [online] Available: http://handle.itu.int/11.1002/ls/sp16-3gpptsgsa4-iLS-00036.zip. [Accessed 2019-11-20] . .

46. FCC Adopts a Second Wave of Millimeter Wave Regulations to Support Next Generation Terrestrial Systems and Services, [online] Available: https://www.commlawmonitor.com/2017/12/articles/wireless-2/fcc-adopts-a-second-wave-of-millimeter-wave-regulations-to-support-next-generation-terrestrial-systems-and-services/. [Accessed 2019-11-20] . .

47. Ghafoor S, Hanzo L. Sub-Carrier-Multiplexed Duplex 64-QAM Radio-over-Fiber Transmission for Distributed Antennas. *IEEE Communications Letters* 2011; 15(12): 1368-1371. doi: 10.1109/LCOMM.2011.101711.111794

48. Wiberg A, Perez-Millan P, Andres MV, Andrekson PA, Hedekvist PO. Fiber-optic 40-GHz mm-wave link with 2.5-Gb/s data transmission. *IEEE Photonics Technology Letters* 2005; 17(9): 1938-1940. doi: 10.1109/LPT.2005.853035

49. Spinnler B. Equalizer Design and Complexity for Digital Coherent Receivers. *IEEE Journal of Selected Topics in Quantum Electronics* 2010; 16(5): 1180-1192. doi: 10.1109/JSTQE.2009.2035931

50. Faruk MS, Kikuchi K. Adaptive frequency-domain equalization in digital coherent optical receivers. *Opt. Express* 2011; 19(13): 12789–12798. doi: 10.1364/OE.19.012789

51. Meher PK, Stouraitis T. *Arithmetic Circuits for DSP Applications*. Wiley-IEEE Press . 2017.

52. Haykin S. *Adaptive Filter Theory, 3rd ed.* Prentice Hall . 2001.

53. Santhosh L, Thomas A. Implementation of radix 2 and radix 22 FFT algorithms on Spartan6 FPGA. In: Fourth International Conference on Computing, Communications and Networking Technologies (ICCCNT); 2013: 1-4

54. Chagnon M, Osman M, Poulin M, et al. Experimental study of 112 Gb/s short reach transmission employing PAM formats and SiP intensity modulator at 1.3 μm . *Optics Express* 2014; 22(17): 21018–21036.

55. Arik SO, Ho K, Kahn JM. Delay Spread Reduction in Mode-Division Multiplexing: Mode Coupling Versus Delay Compensation. *Journal of Lightwave Technology* 2015; 33(21): 4504-4512. doi: 10.1109/JLT.2015.2475422

56. Xiong W, Hsu C, Bromberg Y, Antonio-Lopez J, Correa R, Cao H. Complete Polarization Control in Multimode Fibers With Polarization and Mode Coupling. *Light Science and Applications* 2018; 56(7).

57. Xia C, Chand N, Velazquez-Benitez AM, et al. Demonstration of world's first few-mode GPON. In: The European Conference on Optical Communication (ECOC); 2014: 1-3

AUTHOR BIOGRAPHY

Saeed Iqbal received his M.Sc degree in Electronics from Quaid-e-Azam University in 2005 and completed his MS in Electronic Engineering from MAJU University, Islamabad in 2010. He is currently pursuing doctoral degree in Electrical Engineering at COMSATS University, Islamabad, Pakistan. From Feburary 2013 to date, he is working as an Assistant Professor at Department of Computer Science, Barani Institute of Information Technology, Rawalpindi, Pakistan. He is an active member of Next Generation Communications Research Group in the Department of Electrical and Computer Engineering, COMSATS University Islamabad. His research interests include channel modeling, MIMO, millimetre Wave technology and radio-over-fiber network design.

Aadil Raza obtained MSc degree in Electronics from the Quaid-i-Azam university, Islamabad, Pakistan in 2005. He received MS degree in Nanoelectronics and Mechanics from The University of Sheffield, United Kingdom in 2009. He completed his PhD in Electrical Engineering from COMSATS University Islamabad, Islamabad, Pakistan in 2019. Currently, he is serving as an Assistant Professor in the Department of Physics, COMSATS University Islamabad, Pakistan since 2007. His areas of research are Radio over Fibre systems, free space optics, chaotic secure communication and advanced digital signal processing (ADSP) to realize high speed short range optical links.

Muhammad Fasih Uddin Butt received B.E. degree from National University of Sciences and Technology (NUST), Pakistan in 1999. He received his M.E. degree from University of Engineering and Technology Taxila, Pakistan with specialization in Digital Communication/Computer Networks in 2003 and his Ph.D. in Electronics and Electrical Engineering from School of Electronics and Computer Science, University of Southampton, U.K in June 2010. Currently, he is a Tenured Associate Professor and the Head of Next Generation Communications Research Group in the Department of Electrical and Computer Engineering, COMSATS University Islamabad, Pakistan where he has been serving as an academic since 2002. His research interests include channel coding, cooperative cognitive radio networks, mm Wave radio-over-fiber technologies, physical layer security, quantum communications and frequency selective surfaces. He has published over 35 research papers in various reputed journals and conference proceedings.

Salman Ghafoor received BSc Electrical Engineering degree from UET Peshawar, Pakistan in 2006. In 2007, he received MSc degree in Electronic Communications and Computer Engineering from University of Nottingham, UK. Dr. Salman worked for 2 years as a research student at the Optoelectronics Research Centre (ORC), University of Southampton, UK. In 2010, he joined the School of Electronics and Computer Science (ECS), University of Southampton where he completed his PhD degree in 2012. Currently, Dr. Salman is working at NUST, Pakistan. His areas of research are optical signal regeneration, wavelength conversion and radio over fiber systems.

Mohammed El-Hajjar is an Associate Professor in the department of Electronics and Computer Science in the University of Southampton. He received his PhD in Wireless Communications from the University of Southampton, UK in 2008. Following the PhD, he joined Imagination Technologies as a design engineer, where he worked on designing and developing Imagination's multi-standard communications platform, which resulted in several patents. He is the recipient of several academic awards and has published a Wiley-IEEE book and in excess of 80 IEEE journal and conference papers. Mohammed's research interests include the design of intelligent and energy-efficient transceivers, cross-layer optimization for large-scale networks, MIMO, millimeter wave communications and Radio over fiber network design.